Journal of ELECTRICAL ENGINEERING, VOL. 63, NO. 5, 2012, 303–309

ELIMINATION OF HARMONIC INDUCED VIABLE BIFURCATIONS WITH TCSC FOR AC–FED ELECTRIC ARC FURNACES

Metin Varan — Yılmaz Uyaroğlu *

AC-fed electric arc furnaces (EAFs) are known with their unbalanced, excessively nonlinear and time varying load characteristics. The nonlinear oscillations produced by EAF operation cause several problems to interconnected feed system. Injection of harmonics/interharmonics and rising flicker effects on the feed system are two of major problems produced by EAF. These nonlinear effects result into quasistatic changes in the feed system parameters $(L - R)$. In last decade many studies have been reported that such quasistatic changes in the feed system parameters result in viable bifurcation formations which strictly cause sudden and drastic changes on system behaviors. This paper presents an analytical control procedure to eliminate viable bifurcation points on $L - I$ and $R - I$ curves that cause sudden resonant peak arc currents. After control procedure, stability margins of EAF are extended into larger levels and viable bifurcation points on the feed system parameter have been eliminated. During study, possible roles of small parameter changes of uncontrolled EAF around bifurcation points and controlled EAF have been traced over time series analysis, phase plane analysis and bifurcation diagrams. A wide collection of useful dynamic analysis procedures for the exploration of studied arc furnace dynamics have been handled through the AUTO open-source algorithms.

K e y w o r d s: viable bifurcation points, elimination, AC-fed electric arc furnaces, nonlinear oscillations, thyristor controlled series compensator (TCSC)

1 INTRODUCTION

Nonlinear loads are the principal cause of power quality problems including voltage dips, harmonic distortion and flicker [1,2]. By this context, AC-fed electric arc furnace (EAF) should be categorized into an unbalanced, excessively nonlinear and time varying load. The nonlinear oscillations produced by EAF operation cause several problems to interconnected feed system. Injection of harmonics and interharmonics to the feed system, unbalanced three phase currents and voltages due to the random nature of the electric arc and erosion of three-phase electrodes, current variations due to the rapid changes in arc lengths and transient oscillations caused by the random movement of the melting material can be expressed into major ones of such these problems. By its external effects on feed systems, EAF also accommodates very sensitive internal peculiarities. Any change from the system parameters results into significant changes in the behaviour of complete system dynamics [3]. Such parameter changes sometimes may result into different degrees of complexity. Dynamical behaviours behind such highly nonlinearities have not been completely understood until now. Moreover, the numerical analysis of the dynamic behaviour of such systems is often cumbersome, especially for systems with many degrees of freedom. The need for accurately understanding about dynamical behaviours of smelting processes, several electric arc furnace models have been developed [4,5,10,13]. Dynamic model representation should be encoureged also with nonlinear dynamic analysis methods. Among several nonlinear mathematical theories, bifurcation analysis method is chosen for investigating qualitatively the ways in which instabilities can take place in EAF.

Bifurcation theory has been widely used to investigate dynamic behaviours of nonlinear components, and to make analytical answers on formation of synchronous resonance, chaotic oscillations and ferroresonance oscillations phenomenon in electrical engineering. Beyond mentioned fields, this theory has been also applied to examine the dynamical behavior of nonlinear components such as induction machines, load models, tap changing transformers, power system stabilisers and static VAR compensators.

Bifurcation theory is also one of the main techniques used to perform stability studies in nonlinear systems. This study aims for demonstrating relationships between formation of bifurcation dynamics and formations of nonlinear oscillations [6] produced by EAF. The paper spesifically focuses as the feed system parameters changing and/or the feed system component parameters' uncertainty may cause significant variations of the nodal equivalent impedances and consequently of the harmonic and interharmonic voltages [7]. After detection of bifurcation formation on feed parameters, system is supported by a control scheme that holds line impedances into stability margins. During study, possible roles of small parameter changes of sample arc furnace system around bifurcation points has been traced over time series analysis, phase plane analysis and bifurcation diagrams.

* Sakarya University Engineering Faculty - Electrical and Electronics Engineering Department - 54100 Esentepe Campus Sakarya, Turkey, mvaran@sakarya.edu.tr, uyaroglu@sakarya.edu.tr

DOI: 10.2478/v10187-012-0044-4, ISSN 1335-3632

This paper is organized as the follows. In Section 2, complicated dynamical behavior of the nonlinear AC-fed electric arc furnace model is further investigated. Arc furnace harmonics and destructive effects are discussed deeply in context of their effects on feed system parameters' change in Section 3. Section 4 discusses extent of bifurcation theory in respect of stability analysis purposes. In Section 5, design principles of thyristor controller series compensator are explained. Section 6 comprises effects of designed control scheme on studied arc furnace system through an after/before control comparative point of view in context of bifurcation dynamics and stability. A brief conclusion of study is presented in last section.

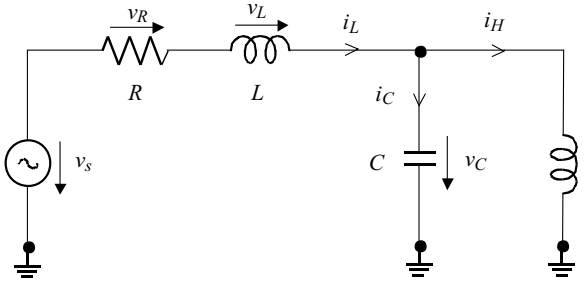

Fig. 1. Schematic diagram of the AC-Fed Arc Furnace Model

2 MODELLING THE AC–FED ARC FURNACE

Electric arc furnaces (EAFs) are used in the production of aluminum, copper, lead, high-grade alloy steel, and other metals. EAFs are large, concentrated, dynamic, and time varying loads [8] and comprise a major portion of industrial loading on the bulk power system. Electric arc furnaces generally are classified by their feed types [9]. AC EAFs are fed by AC source which connected to furnace electrodes via a transformer, whereas DC EAFs connected to electrodes via DC rectifier. In this work AC EAF is considered as case study.

Based on energy conservation, the power balance for the arc can be written as [14], $p_1 + p_2 = p_3$ where

$$p_1 = K_1 r^n \tag{1}$$

accounts for the power transmitted in the form of heat to the external environment with: $n = 0$ if there is non-dependence of the arc temperature on the arc radius, $n = 1$ in the case of a long arc and cool medium covering the arc, while $n = 2$ represents the arc cooling proportional to the electrode cross-section. Further terms represent the power which increases the internal energy in the arc and therefore affects its radius (p_2) – this is proportional to the time derivative of the energy inside the arc which is proportional to r – and the total power developed in the arc and transferred into heat (p_3)

$$p_2 = K_2 r \frac{dr}{dt}, \qquad p_3 = vi = K_3 i^2 r^{(m-2)} \tag{2,3}$$

here K_1, K_2, K_3 are the constants of the arc cooling effects which is supposed to be a function of the arc radius-r only. Exponent m again accounts for the inner temperature effect and is: $m = 0$ for a large and colder arc length, or $m = 2$ for a smaller and hotter arc length, whereas $m = 1$ represents the intermediate length and temperature. Thus

$$K_1 r^n + K_2 r \frac{\mathrm{d}r}{\mathrm{d}t} = \frac{K_3}{r^{m+2}} i^2 \tag{4}$$

Figure 1 illustrates an AC-fed arc furnace connected to a power network. Here, R and L represents the resistance and inductance of the power system, respectively, V_S shows magnitude of the AC feed, V_R and V_L holds the associated voltages, C is the capacitor bank connected parallel with the electric arc furnace, V_C is the voltage across the capacitor bank, L_H is the equivalent inductance of the flexible connection cables, the electric arc furnace transformer and the electrodes [11].

After coupling modeled arc furnace in (4) to the network and appliance of Kirchhoff's current and voltage laws to the meshes and nodes of the circuit sketched in Fig.1, following state equations can be written

$$\begin{aligned}
\frac{\mathrm{d}iq_L}{\mathrm{d}t} &= -\frac{R}{L} i_L - \frac{1}{L} v_C + \frac{1}{L} v_S \\
\frac{\mathrm{d}v_C}{\mathrm{d}t} &= \frac{1}{C} v_C - \frac{1}{C} i_H \\
\frac{\mathrm{d}i_H}{\mathrm{d}t} &= -\frac{1}{L_H} v_C - K_3 \frac{r^{-(m+2)}}{L_H} i_H \\
\frac{\mathrm{d}r}{\mathrm{d}t} &= K_3 \frac{r^{-(m+3)}}{K_3} i_H - K_1 \frac{r^{(n-2)}}{K_2} r
\end{aligned} \tag{5}$$

Here the state variables of system are i_L - current magnitude of inductor, v_C - voltage magnitude across capacitor bank, i_H - current magnitude flows into arc furnace electrodes, and r – is the radius of the arc furnace. During the analysis process the effect of the internal furnace refractory is ignored and K_1=0.08, K_2=0.005 and K_3=3.0 as fixed parameter for nominal operation points for arc furnace [11, 14].

3 ARC FURNACE HARMONICS AND DESTRUCTIVE EFFECTS

Power system harmonics are integer multiples of the fundamental power system frequency and basically are created by non-linear devices connected to the power system. The harmonics has adverse effects on both the power utility and the power consumer which includes transformers overload and failure of capacitor banks among other immense effects.

By this context, AC-fed electric arc furnace (EAF) should be categorized into an unbalanced, excessively nonlinear and time varying load that accommodates very impressive harmonics. Because of the non-linear resistance, an arc furnace acts as a source of current harmonics of the second to seventh order, especially during

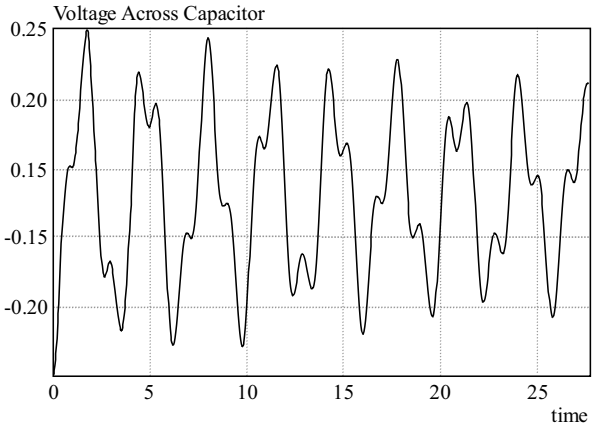

Fig. 2. Voltage across capacitor parallel connected across the AC-fed arc furnace

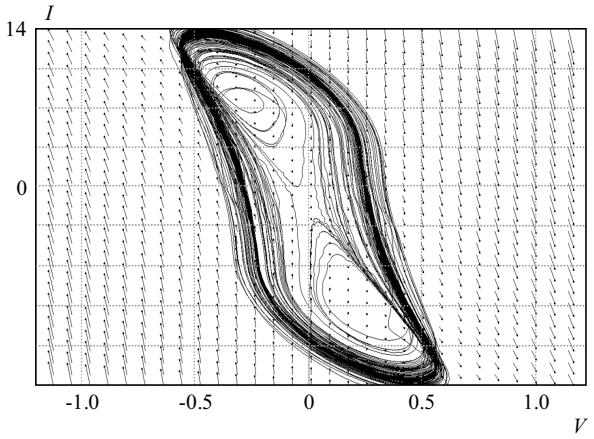

Fig. 3. $V - I$ Characteristic of studied AC-fed arc furnace

the meltdown period. Voltage fluctuations are produced, in this way through impedance on the value of harmonic currents supplied and the effective impedances at the harmonic frequencies. Fig.2 depicts harmonics over voltage parameter of studied EAF.

Current harmonics have their origin in the nonlinear voltage-current characteristics of the arc voltage [12]. Figure 3 sketches phase plane diagram for nonlinear $V - I$ characteristics of studied EAF. As previously expressed in section-2, the parameters in (4) have a direct effect on the convergence speed to the overall system stability, the arc $V - I$ characteristics and on its equilibrium operation points.

Heating effects of harmonics in distribution system components are capacitor and insulation failure due to harmonic resonance, malfunction of installed protection systems, transient voltage fluctuations, over heating of system transformer and cables, error of power electronic equipment operations. Let the following equation describe the resistance changes with the temperature.

$$R = R_0\big(1 + a(T_{\text{final}} - T_{\text{init}})\big) \tag{6}$$

The network configuration changing and/or the network component parameter uncertainty may cause significant variations of the nodal equivalent impedances and consequently of the harmonic and inter-harmonic voltages.

$$\begin{aligned} X_L &= j2\pi fL \\ X_C &= -j/2\pi fC \\ Z &= R + j(X_L||X_C) \end{aligned} \tag{7}$$

Power system impedance is inductive and increases with frequency, consequently the higher frequency components of current give a correspondingly greater distortion in the voltage waveform. On the other hand capacitors have impedance which reduces with frequency [13]. Equations (7) show the impedance relations of an inductor and a capacitor with the system frequency. The combined effect of the two is the following:

- at low frequencies, the impedance of the power system is determined by the low inductive impedance of transformer and transmission lines
- at high frequencies, it is determined by the low capacitive impedance of power factor correction capacitors

Installing capacitor bank parallel with furnace bus is one of the preventive techniques for harmonic sourced problems. On the other side, due to interaction with varying feed parameters, the presence of capacitor bank may convey harmonic disturbances into dangerous levels. At certain frequencies, resonance exists between the capacitor bank and the reactance of the feed seen from the bank terminals.

4 BIFURCATION THEORY

Dynamical systems commonly arise when one formulates equations of motion to model a physical system. The setting for these equations is the phase space or state space of the system. A point x in phase space corresponds to a possible state for the system, and in the case of a differential equation the solution with initial condition x defines a curve in phase space passing through x. The collective representation of these curves for all points in phase space comprises the phase portrait. This portrait provides a global qualitative picture of the dynamics, and this picture depends on any parameters that enter the equations of motion or boundary conditions [15]. If one varies these parameters the phase portrait may deform slightly without altering its qualitative (*ie*, topological) features, or sometimes the dynamics may be modified significantly, producing a qualitative change in the phase portrait. Bifurcation theory studies these qualitative changes in the phase portrait, *eg*, the appearance or disappearance of equilibria, periodic orbits, or more complicated features such as strange attractors. The knowledge of the bifurcation structure of a dynamical system is therefore important in order to understand the system response to the changes in parameter values. The methods and results of bifurcation theory are fundamental to an understanding of nonlinear dynamical systems [15].

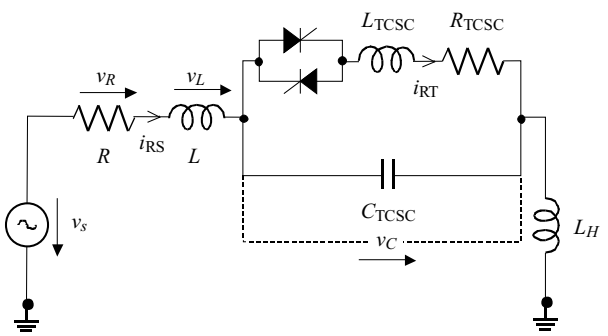

Fig. 4. Schematic diagram of the AC-fed arc furnace model with TCSC installation

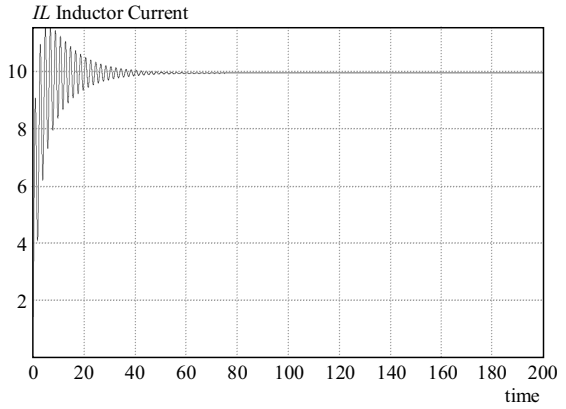

Fig. 5. After stabilization of the arc furnace inductor current

The system stability analysis based on the bifurcation approach requires of a set of differential and/or algebraic equations which contain two type of variables; state and parameters. In this study, the EAF dynamic model is only characterized by a set of parameter dependent differential equations, that is

$$\dot{x} = f(x, \lambda) \tag{8}$$

where $x \in \Re^n$ is a vector of the dynamic state variables, and $\lambda \in \Re^k$ is a vector of system parameters which change slowly, moving the system from one equilibrium point to another. In this paper we restrict k to be one, such that λ is a scalar [15].

For the state equations of system given in 13), let the equilibrium point be $P_e = (x_e, \lambda)$, the Hopf bifurcation takes place when the following condition is satisfied

- The Jacobian matrix- $\mathbf{J}_x$ has a simple pair of pure imaginary eigenvalues; ie, $\gamma(\lambda_e) = \alpha(\lambda_e) \pm j\omega(\lambda_e)$ such that $\alpha(\lambda_b) = 0$ and $\omega(\lambda_b) > 0$, and there are no other eigenvalues with zero real parts
- $\frac{\mathrm{d}\ \mathrm{Re}\,\gamma(\lambda)}{\mathrm{d}\lambda}|_{\lambda=\lambda_c} \quad \frac{\mathrm{d}\alpha(\lambda)}{\mathrm{d}\lambda}|_{\lambda=\lambda_c \neq 0}$

A Hopf bifurcation is characterized by the emergence of a small-amplitude periodic orbit (limit cycle) from an equilibrium point when a system parameter is changed. Whether this oscillatory behavior entails small or growing oscillations depends of whether the bifurcation is super-critical or sub-critical, respectively [16]. The former occurs when a stable limit cycle coalesces with an unstable equilibrium point; hence, the periodic orbit emerges for parameter values at which the equilibrium point has lost stability. In this case, the solution trajectories converge to a small-amplitude periodic solution. A sub-critical hopf bifurcation occurs when an unstable limit cycle coalesces with a stable equilibrium point. Therefore, the periodic orbit appears for parameter values at which the equilibrium point is stable. In this case, the amplitude of the oscillatory behavior increases unboundedly.

5 THYRISTOR CONTROLLER SERIES COMPENSATOR (TCSC) MODEL CONNECTED WITH ARC FURNACE

Thyristor Controlled Series Compensator (TCSC) is one of the important members of FACTS family that is increasingly applied with long transmission lines by the utilities in modern power systems [17]. As shown in Fig. 4, the studied system is compensated by a TCSC that consisting of a fixed capacitor in parallel with a thyristor controlled reactor and connected to a firm voltage source. The TCSC is controlled by varying the phase delay of the thyristor firing pulses synchronized through a PLL to the line current waveform.

Modeled TCSC has three operation modes; bypassed thyristors mode, blocked thyristors mode, and Vernier mode, respectively [18]. In Vernier mode, dynamic operation of the modeled TCSC is achieved with the continuous variation of the thryristors firing angle.

By insight of meshes and current directions, proper application of the KVL and KCL to the meshes and nodes of the circuit of Fig. 4 following state equations can be written

$$\begin{aligned}
\frac{\mathrm{d}i_{RS}}{\mathrm{d}t} &= -\frac{R_1}{L_1} i_{RS} - v_C + v_S \\
\frac{\mathrm{d}i_{RT}}{\mathrm{d}t} &= -\frac{R_T}{L_2} i_{RT} + S(t) v_C \\
\frac{\mathrm{d}v_C}{\mathrm{d}t} &= \frac{1}{L_s C_1} i_{RS} + -\frac{S(t)}{L_T C_1} i_{RT}
\end{aligned} \tag{9}$$

Dynamic analysis of studied TCSC installed arc furnace system has been handled by combining TCSC state equations and arc furnace state equations based on the model reported by Acha [14], Martinez [10], and Medina [18].

6 BIFURCATION DYNAMICS OF STUDIED ARC FURNACE MODEL

In this part of study, outputs of detailed bifurcation dynamics of studied arc furnace model with/without

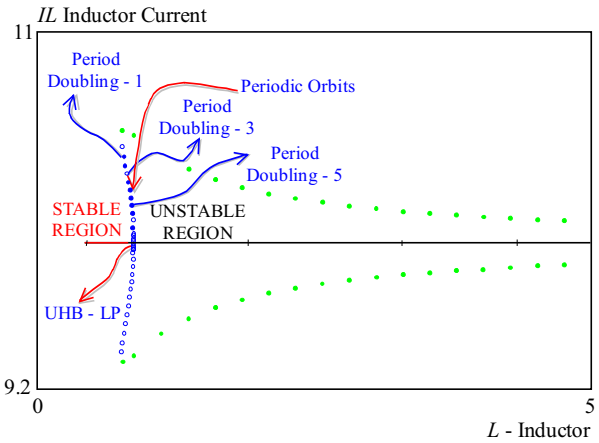

Fig. 6. $(iL - L)$ Bifurcation diagram of AC-fed arc furnace before TCSC

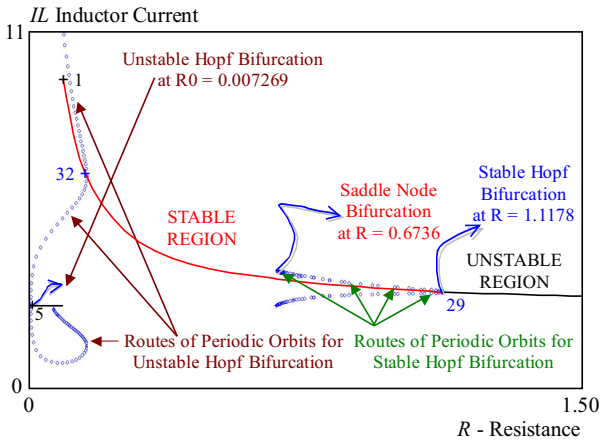

Fig. 7. $(iL - R)$ Bifurcation diagram of AC-fed arc furnace before TCSC

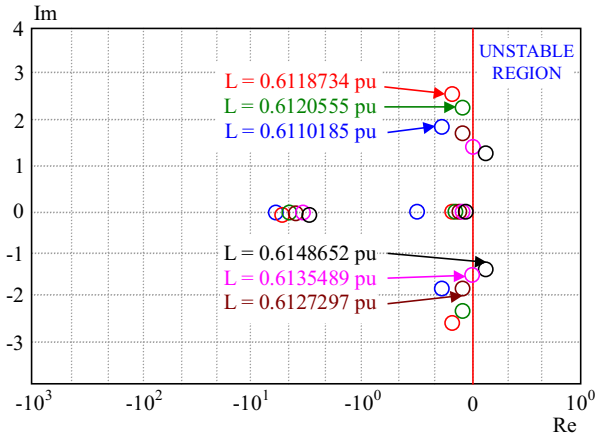

Fig. 8. Changes of eigenvalues at equilibrium point of system before TCSC

TCSC are presented. It is important to remark that system parameters are selected around industrial operation ranges [Appendix]. Any variation on the system parameters can potentially define a different equilibrium point [11]. These parameters correspond to a stable equilibrium point of the network, as shown in Fig.5, which illustrates the system transient behavior until it eventually reaches the steady state in $t = 48$ ms with $i = 10.6298$.

6.1 Dynamics before TCSC installation

With initial conditions, the system will be shown by $\dot{I}_0 = (i_{L0}, v_{C0}, i_{H0}, r_0, L)$ Initial conditions parameters are respectively:

And, initial conditions parameters are taken $I_0 = (10.6298, 0.315, 0.00134, 0.932177, 0.120)$. In this paper, bifurcation points are identified through combined assessment of eigenvalues. Her L is chosen as bifurcation parameter. In Fig.6, the bifurcation points are shown by PDB-1, PDB-3, PDB-5 and UHB-LP abbreviations.

As shown in Fig.6, bifurcation diagram demonstrates change of i_L -inductor current in regard with change of inductance of feed. From PDB-1 to PDB-5 the system oscillates around stability margins.

Table-1 includes initial values of (i_L, v_C, i_H, r, L) state variables and bifurcation parameter L in the course of bifurcation points. Unstable/supercritical Hopf bifurcation point is detected at $L = 0.613548$. Real part of conjugate eigenvalues at UHB point is out of stability margins borders. At that point Lyapunov coefficient calculated as positive value which confirms chaotic nature. Figure 7 sketches bifurcation diagram demonstrates change of iL-inductor current in regard with change of resistance of feed. Until $R = 0.101845$, allover system fails unstable margin. At $R = 0.007269$, UHB point is detected. Periodic orbits route of that point is shown in Fig.7. After $R = 0.101845$ system starts to be pushed into stable margin. This stability intervals continue until $R = 1.1178$. While tracing periodic orbits route of that point, it is shown that system initials like at R=0.6736 value impress to fail a SNB (Saddle Node Bifurcation) point which convey system state in a critical region again.

Table 1. Bifurcation point types and typical values

Bifurcation name	Initial values (i_L, v_c, i_H, r, L)	First Lyapunov coefficient
PDB-1	(9.24394,0.66317,) (11.40363,5.44987,0.6118734)	-93.589
PDB-3	(9.3145056,0.538464,) (11.03236,5.38086,0.6120555)	-19.645
PDB-5	(9.46237,0.25699,) (10.20492,5.222250,0.612729)	-5.965
UHB-LP	(9.57417,0.04054,) (9.596,5.09620,0.613548)	1.245×10^{-4}

Figure 4 depicts the changes of relevant eigenvalues of PDB-1, PDB-3, PDB-5 and UHB-LP at equilibrium points. The eigenvalues are calculated by values of the system equilibrium points into values of state variables in the Jacobian matrix [19]. There are four eigenvalues for each equilibrium point because of the system representation by the four first order state equations.

At $L = 0.61065$, the eigenvalues are $(e_{1,2} = -0.172j2.02, e_3 = -0,149, e_4 = -7,99)$. It is clear that eigenval-

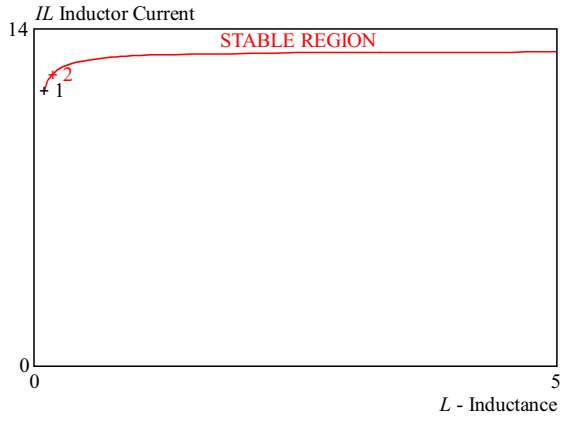

Fig. 9. $(i_L - L)$ Bifurcation diagram of AC-fed arc furnace after TCSC

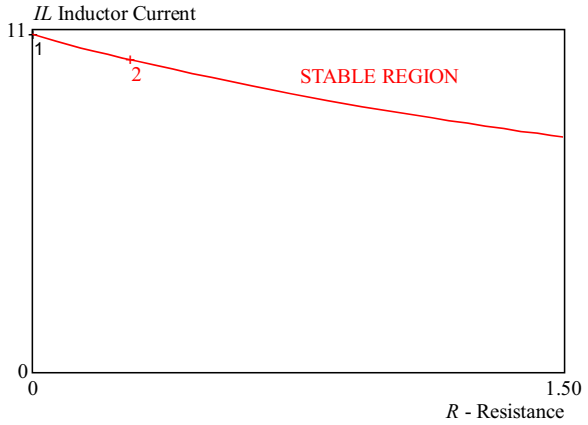

Fig. 10. $(i_L - R)$ Bifurcation diagram of AC-fed arc furnace after TCSC

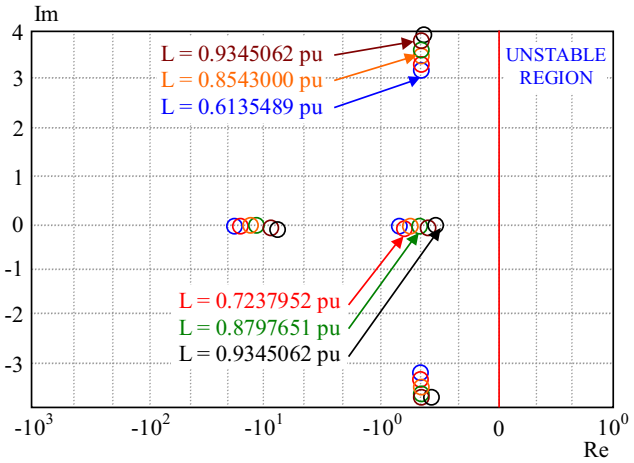

Fig. 11. . Changes of eigenvalues at equilibrium point of system after TCSCC

ues at that point are far from instability margin. At L =0.61188 (PDB-1) value, the eigenvalues are $(e_{1,2} = -0.153 \pm j2.56, e_3 = -0,085, e_4 = -7,52)$. At =.61206 (PDB-3), the eigenvalues are $e_{1,2} = -0.148 \pm j2.22, e_3 = -0,057, e_4 = -6,80)$. At L =0.61273 (PDB-5) value, the eigenvalues are $(e_{1,2} = -0.082 \pm j1.93, e_3 = -0,048, e_4 = -5,65)$. It is clear that eigenvalues from PDB-1 to PDB-5 draw near stability margin border. At L =0.613548 (UHB-LP) value, the eigenvalues are $(e_{1,2} = 0.00004 \pm j1.37,\ e_3 = -0,035, e_4 = -4,28)$. For this point necessary condition for Hopf bifurcation is satisfied by the presence of complex conjugate eigenvalues with real part Re[2] 0 and Re[3] 0. Real part of conjugate eigenvalues at UHB point spills over into stability margins borders.

6.2 Dynamics after TCSC installation

Initial conditions parameters are taken I_0= (11.4178, -0.02381, 13.75649, 3.549355, 0.120). Parameters of studied arc furnace model with TCSC are given in Appendix-B. It is important to remark that system parameters are selected around industrial operation ranges.

As shown in Fig.9, bifurcation diagram demonstrates change of iL-inductor current in regard with change of inductance of feed system. After TCSC control scheme, bifurcation points on L-I curve that cause sudden resonant peak arc currents have been eliminated. Fig.10 sketches bifurcation diagram of iL-inductor current in regard with change of resistance of feed system. After TCSC control scheme, bifurcation points on R-I curve have been eliminated. Stability margins of EAF have been extended into larger levels.

Figure 11 depicts the changes of relevant eigenvalues for different L-values at equilibrium points. The eigenvalues are calculated by values of the system equilibrium points into values of state variables in the Jacobian matrix [19]. It is clear that eigenvalues at all points are very far from unstability margin. Results sketched into Fig.9-10 and 11 proved that designed TCSC extends stability margins of EAF system to larger levels.

7 CONCLUSIONS

This paper presents an analytical control procedure to eliminate viable bifurcation points on L-I and R-I curves that cause sudden resonant peak arc currents. The TCSC possesses positive technical qualifications as it considerably provides control of line impedance, which is a basic power system parameter on which system performance depends [20]. After control procedure, stability margins of EAF have been extended into larger levels and viable bifurcation points on the feed system parameter have been eliminated. During study, possible roles of small parameter changes of uncontrolled EAF around bifurcation points and controlled EAF have been traced over time series analysis, phase plane analysis and bifurcation diagrams. A wide collection of useful dynamic analysis procedures for the exploration of studied arc furnace dynamics have been handled through the AUTO open-source algorithms.

Acknowledgement

This work is supported in part by the Scientific Research Support Program Fund in Sakarya University with grant-number: 2011-50-02-008 (http://www.eee.sakarya.edu.tr/ tr/arastirma_projeleri.)

APPENDIX

Model without TCSC

Parameters:	Initial conditions:
L	0.120
V_s	1
m	2
n	2
K_1	0.08
K_2	0.079199
K_3	3
R	0.1
L_H	0.1

Model with TCSC

Parameters:	Initial conditions:
C_{TCSC}	0.790
L_{TCSC}	0.891
R_{TCSC}	0.0206
R_1	0.0206
L_1	0.447
L_s	0.10

References

[1] YAZDANI, A.—MARIESA, L.—GUO, J.: An Improved Nonlinear STATCOM Control for Electric Arc Furnace Voltage Flicker Mitigation, IEEE Trans. On Power Delivery **24** No. 4 (2009), 2284–2290.

[2] WANG, Y. F.—JIANG, J. G.—GE, L. S.—YANG, X. J.: Mitigation of Electric Arc Furnace Voltage Flicker using Static Synchronous Compensator, Proc. IEEE Power Electronics and Motion Control Conf No. 3 (2006), 1–5.

[3] ROSEHART, W. D.—CAN, C. A.—ZARES, I.: Bifurcation Analysis of Various Power System Models, Int. J. Elect. Power Energy Syst. **21** No. 3 (1999), 171–182.

[4] HAN, C.—YANG, Z.—CHEN, B.—HUANG, A.—ZHANG, B.—INGRAM, M.—EDRIS, A. A.: Evaluation of Cascade-Multilevel-Converter-based STATCOM for Arc Furnace Flicker Mitigation, IEEE Trans. Ind. Appl. **43** No. 2 (2007 378-385).

[5] SAMET, H.—GOLSHAN, M. EH.: Employing Stochastic Models for Prediction of Arc Furnace Reactive Power to Improve Compensator Performance, IET Gen. Transmission and Distribution **2** No. 4 (505–515).

[6] MITHULANANTHAN, N.—CAN, C.—ZARES, I.—REEVE, J.—ROGERS, G. J.: Comparison on PSSS, SVC and STATCOM Controllers for Damping Power Systems Oscillations, IEEE Trans. Power Syst. **18** No. 2 (2003), 786–792.

[7] TESTA, A.: Network Impedance Uncertainty in Harmonic and Interharmonic Distortion Studies, Journal of PowerTech-Budapest **99** No. 1 (1999), 227–240.

[8] CARRILLO, E. O.—BANFAI, B.—HEYDTH,: EMTP Implementation and Analysis of Nonlinear Load Models, Electric Power Components and Systems **29** No. 1 (2001), 809–820.

[9] YU-JEN, H.—KUAN-HUNG, C.—PO-YI, H.: Electric Arc Furnace Voltage Flicker Analysis and Prediction, IEEE Trans. on Intstrumentation and Measurement **60** No. 10 (2011), 3360–3368.

[10] MEDINA, A.—GARCIA, N.: Newtons Methods for the Fast Computation of the Periodics Steady State Solutions of Systems with Nonlinear and Time-Varying Components, in Conf IEEE PES Summer Meeting, vol. 2, Edmonton-Canada, 1999, pp. 664–669.

[11] MEDINA, A.—GÓMEZ-MARTÍNEZ, C. R.—UERTE-ESQUIVEL: Application of Bifurcations Theory to Assess Nonlinear Oscillations Produced by AC Electric Arc Furnaces, IEEE Trans. On Power Delivery **20** No. 2 (2005), 801–807.

[12] EMANUEL, A. E.—ORR, J. A.: : An Improved Method of Simulation of the Voltage-Current Characteristic, 9th international Conference on Harmonics and Quality of Power, Proceedings, Orlando-Florida, 2000, pp. 148–150.

[13] LINDBLOM, A.—ISBERG, J.—BERNHOFF, H.—LEIJON, M.: Inductive High Voltage Pulse Generator Based On Resonance System, J. Electrical Eng. **58** No. 1 (2007), 19–25.

[14] ACHA, E.—SEMLYN, A.—RAJAKOVICK, N.: : A harmonic Domain Computational Package for Nonlinear Problems and its Applications to Electrics Arcs, IEEE Trans. On Power Delivery **5** No. 1 (1990), 1390–1397.

[15] CRAWFORD, J. D.: Introduction to Bifurcation Theory, Reviews of Modern Physics **63** No. 4 (1991), 991–992.

[16] STROGATZ, H. S.: Nonlinear Dynamics and Chaos, Cambridge-Perseus publishing, 2000.

[17] PANDA, S.: Multi-Objective Non-Dominated Shorting Genetic Algorithm-II For Excitation and TCSC-Based Controller Design, J. Electrical Engineering **60** No. 2 (2009), 86–93.

[18] MEDINA, A.—RAMOZ-PAZ, A.—FUERTE-ESQUIVEL, C. R.: Swift Computation of the Periodic Steady State Solution of Power Systems Containing TCSCs, Electrical Power and Energy Systems **25** No. 3 (2003), 689–694.

[19] DU-QU, W.—XIAO-SHU, L.—BO, Z.: Noise-Induced Voltage Collapse in Power Systems, China Physics Letters.

[20] ALOMOUSH, M. I.: : Multicriteria Selection Of Optimal Location Of TCSC In A Competitive Energy Market, J. Electrical Engineering **61** No. 3 (2010), 129–140.

Received 27 April 2011

Metin Varan was born 1981 in Bingöl, Turkey. He has graduated from Sakarya University Electrical & Electronics Engineering department in 2006. He has received MS degree n 2008 from Sakarya University of Electrical & Electronics Engineering. Currently working as a senior software developer specialist at Computer Sciences Research and Application Centre in Sakarya University after compleed PhD study at Electrical Engineering Department in Sakarya University. His interests are basically in Electric Power System Analysis, Stability Analysis in Power Systems, Application of Bifurcation and Chaos Theory in Electric Engineering, Power System Software Methodologies, and Effective Data Collecting Algorithms in Smart Grids, Embedded System Programming, API Programming, and Object Oriented Programming.

Yılmaz Uyaroğlu was born 1966 in Adapazarı, Turkey. He has graduated from Istanbul Technical University Electrical & Electronics Engineering department in 1989. After getting MS degree from Sakarya University he gained his PhD degree at the same in 2002. Afterward he has studied as post-doc researcher at Hochschule Fr Technik Zrich in Swiss-2006. His interests are basically in Electric Power System Analysis, Voltage Stability Analysis in Power Systems, Application of Bifurcation and Chaos Theory in Electric Engineering, Chaotic Communication Circuits. Currently, he is a faculty member at Electrical & Electronics Engineering Department.